Rayleigh-Bénard convection at Pr=120 and Ra=10^6 in a large aspect ratio domain

By T. Hartlep AND J.-F. Ripoll†

Three-dimensional Rayleigh-Bénard flow is computed at Pr = 120 and Ra = 10^6 in a domain of aspect ratio 10. Geometry, thermal conditions, and fluid properties are chosen to be similar to those of low viscosity glass melting in a furnace. A solution is obtained with Fluent and is compared with results from a reference code. Rather good agreement is found and the computed flow patterns are discussed.

1. Introduction

Engineers often use commercial codes, such as Fluent, to compute complex flows involved in their processes of interest. It is then important to have reference cases to assess the accuracy of such simulations for these problems. We choose here an academic problem of natural Rayleigh-Bénard convection at high Prandtl number (Pr = 120) and high Rayleigh number (Ra = 10^6) for a simple $10\,\mathrm{m} \times 10\,\mathrm{m} \times 1\,\mathrm{m}$ domain. The fluid properties and dimensions are common in the glass manufacturing process, in which melted glass can assume Prandtl numbers between about 10 and 600 and is subject to forced and natural convection processes at high Rayleigh numbers.

Convection in a glass furnace is mainly driven by differential heating along the top. At the glass surface, horizontal temperature gradients, resulting from the presence of cold batch (fresh glass material entering the furnace) on one side and hot molten glass elsewhere, create natural convection. Wang & Huang (2005) show experimentally that such a flow is very steady, stable, and driven by the boundary layer, confirming the fundamental results of Rossby (1965). It is also theoretically understood in two dimensions (J.-M. Flesselles & F. Pigeonneau 2004; Chiu-Webster et al. 2008). The Rayleigh-Bénard instability is thus not likely to happen in the furnace as a whole, but it can take place for particular conditions or locations, for instance underneath the batch (Pillon et al. 2002).

In this paper we consider Rayleigh-Bénard convection at fixed Rayleigh and Prandtl numbers. This is simpler than real molten glass in which, for instance, the temperature dependence of the viscosity and thermal conductivity (accounting for radiative heat transfer) is important. Still, this case can serve as a test for the simulation methodology since it involves sharp gradients and a complex thermal structure. Typically, industrial engineers perform steady-state simulations for such flows, and we wish to assess what accuracy we can expect since they are actually unsteady.

Rayleigh-Bénard convection at high Prandtl numbers has been extensively studied in the past (e.g., Busse 1967; Busse & Whitehead 1974; Busse 1979; Frick et al. 1983; Hansen et al. 1990; Koschmieder 1993; Hartlep et al. 2003). Convection produces a wide variety of flow patterns, well known examples being atmospheric mesoscale convection, or the solar granulation (Stein & Nordlund 1998; Stein et al. 2004, and references in them). In

† Saint-Gobain Recherche, Aubervilliers, France

our high Prandtl number regime, the tendency towards polygonal convection cells, which is observed at lower Prandtl numbers, is no longer evident. Instead, for $Ra = 10^4$ and higher, one encounters flows which have been called spoke-pattern convection (Busse & Whitehead 1974) in which, as we will show below, the convective structure appears to be governed by central plumes which are fed by spoke-like ridges of hot and cold fluid confined in their respective boundary layers. These flows are intrinsically unsteady and involve a wide range of spatial and temporal scales.

2. Formulation of the problem

We consider the classic Rayleigh-Bénard problem: a horizontal fluid layer between two rigid, isothermal plates heated from below and cooled from above. Temperature variations are assumed to be small so that the Boussinesq approximation can be used, and density variations are neglected except in the buoyancy term in which a linear temperature dependence of the density is assumed. The material properties κ (thermal diffusivity), ν (kinematic visocity), and α (volumetric expansion coefficient) are considered constant. The gravitational acceleration g acts in the negative z-direction, in a 3D Cartesian coordinate system. Using the distance d between the plates as a unit of length, the diffusion time d^2/κ as a unit of time, and the temperature difference ΔT between the lower and upper plate as a unit of temperature, we can derive non-dimensional equations for the velocity field $\boldsymbol{v}(\boldsymbol{r}, t)$ and the temperature $T(\boldsymbol{r}, t)$ in the form:

$$\partial_t \boldsymbol{v} + (\boldsymbol{v} \cdot \nabla)\boldsymbol{v} = -\nabla P + \mathrm{Pr}\ \nabla^2 \boldsymbol{v} + \mathrm{Ra}\ \mathrm{Pr}\ T\hat{\boldsymbol{z}}, \tag{2.1}$$

$$\nabla \cdot \boldsymbol{v} = 0, \tag{2.2}$$

$$\partial_t T + \boldsymbol{v} \cdot \nabla T = \nabla^2 T, \tag{2.3}$$

where $\hat{\boldsymbol{z}}$ is the unit vector in z-direction, and all terms that can be written as gradients have been combined with the pressure into the ∇P term. The system of equations is controlled by only two dimensionless numbers: the Rayleigh number $\mathrm{Ra} = g\alpha d^3 \Delta T/(\kappa\nu)$ and the Prandtl number $\mathrm{Pr} = \nu/\kappa$.

We compare the results from two different simulation codes: a research code (referred to as the "reference"), and the commercial CFD software Fluent. The reference code (for a detailed description, see Hartlep & Tilgner 2003) uses a highly efficient spectral method similar to Moser et al. (1983); Kerr (1996), discretizing the z-direction with Chebychev polynomials, and with Fourier modes in the x- and y-directions. Periodic boundary conditions are imposed in the horizontal directions. Resolution for the case presented here is 341×341 Fourier modes and 33 Chebyshev polynomials. A second-order Adams-Bashforth scheme for the advection and buoyancy terms coupled to a Crank-Nicolson scheme for the diffusive terms is used for time advancement. The computation was initiated from random noise and run for several tens of convective time-scales $\tau = (2E_{kin})^{1/2}$, where E_{kin} is the non-dimensional average kinetic energy density.

In the Fluent computations, a zero shear stress is imposed along the sides instead of the periodic boundary conditions used in the reference code. Second order schemes are used in space and time. A computation with 6.25M hexahedric cells ($250 \times 250 \times 100$) was performed, which lasted 70 hours on 16 AMD-64 processors running at 2.6 Ghz. The computation was run for 15000 iterations. The *scaled residuals* remained nearly constant after 5000 iterations and were bounded by 2×10^{-4} for the velocities and by 7×10^{-7} for energy, which are below the Fluent 6.3 user's guide recommendations for convergence to a steady state (10^{-3} and 10^{-6} respectively). However, in monitoring the quantities, we could see the spokes moving slightly (proportionally to the non-zero residuals) and

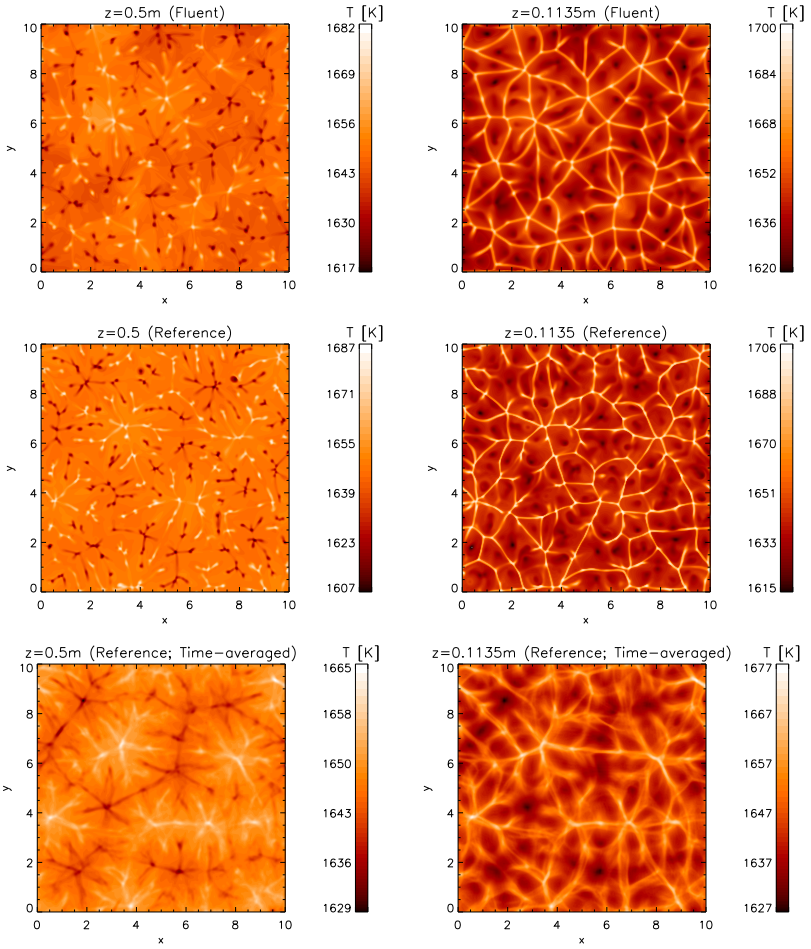

FIGURE 1. Horizontal slices of the temperature at $z = 0.5\,\mathrm{m}$ (*left column*) and at $z = 0.1135\,\mathrm{m}$ (*right column*) for the Fluent solution (*top row*), a snapshot of the reference solution (*center row*), and the time-averaged reference solution (92 mins) (*bottom row*).

temperatures changing by 1 or 2 K, attesting to the actual unsteady character of the flow.

3. Numerical results

The parameters for this study were chosen to be similar to what might be encountered in a glass melting furnace, except for the fact that viscosity and thermal diffusivities are here assumed to be constant. We consider a domain 1 m tall and $10\,\mathrm{m} \times 10\,\mathrm{m}$ wide, i.e. with an aspect ratio of 10. The temperatures at the top and bottom plates are set to $T_1 = 1573\,\mathrm{K}$ and $T_2 = 1723\,\mathrm{K}$, respectively, so that the difference $\Delta T = 150\,\mathrm{K}$. The fluid properties are chosen to be: $\alpha = 7.3 \times 10^{-5}\,\mathrm{K}^{-1}$, $\nu = \mu/\rho = 3.62 \times 10^{-3}\,\mathrm{m}^2/\mathrm{s}$, and $\kappa = \lambda/(C_p\rho) = 3.06 \times 10^{-5}\,\mathrm{m}^2/\mathrm{s}$ with $C_p = 1400\,\mathrm{J/(kg\,K)}$, $\rho = 2366\,\mathrm{kg/m}^3$. This yields a Prandtl number $\mathrm{Pr} = 120$ and a Rayleigh number $\mathrm{Ra} = 10^6$.

In the following we discuss and compare the results obtained with the two simulation codes. Figures 1 and 2 show horizontal cuts of the temperature and vertical velocity,

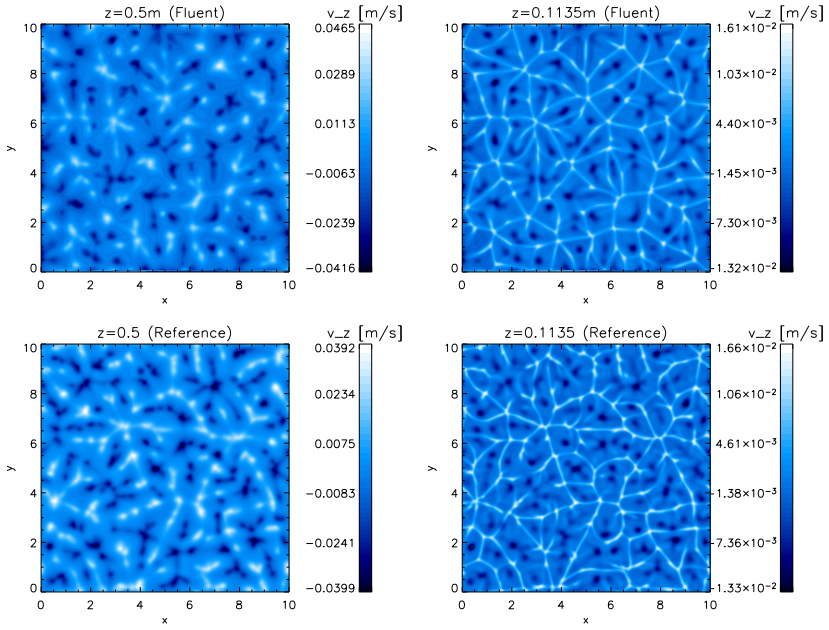

FIGURE 2. Horizontal slices of the vertical velocity at $z = 0.5$ and $z = 0.1135\,\mathrm{m}$ (*left and right column*) for the Fluent solution and a snapshot of the reference solution (*top and bottom row*).

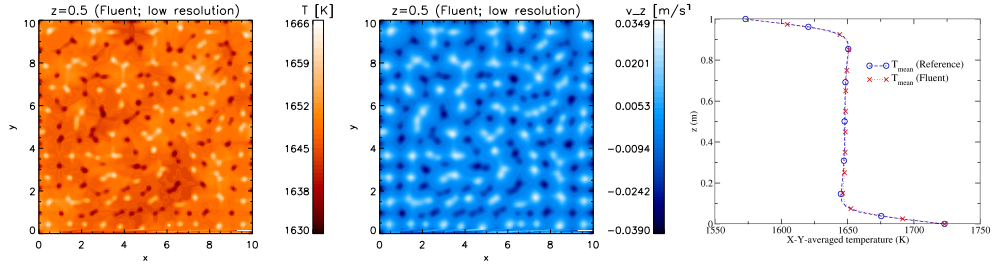

FIGURE 3. Temperature and vertical velocity at $z = 0.5\,\mathrm{m}$ from a lower-resolution (1.5M cells) Fluent simulation (*left and center panel*). Horizontally averaged temperature as a function of z (*rigth panel*) for the Fluent solution (*dotted line*) and the reference simulation (*dashed line*).

respectively, at different heights within the fluid layer for the Fluent simulation as well as for the reference calculation. It is apparent that both the temperature and the velocity fields of the Fluent solution look rather similar to the snapshots from the reference simulation. In the middle of the layer ($z = 0.5\,\mathrm{m}$), the flow is dominated by individual thermal plumes, seen as small hot and cold spots in the horizontal cuts, which are partly connected by so-called spokes. These spokes form a strongly connected network in the boundary layers (see plots at $z = 0.1135\,\mathrm{m}$), but do not extend through the whole fluid layer. Only individual plumes which arise from the spokes can reach the opposite plate. The filamentary structures in these plots are called spokes because they connect to more persistant, central plumes, like spokes in a wheel connect to a central hub. This is less easily seen in snapshots of the flow, but the time-averaged plots (especially at $z = 0.5\,\mathrm{m}$) shown in figure 1 reveal this fact. Over time, most of the plumes in the flow move around with the spokes they arise from, but there are certain regions in the

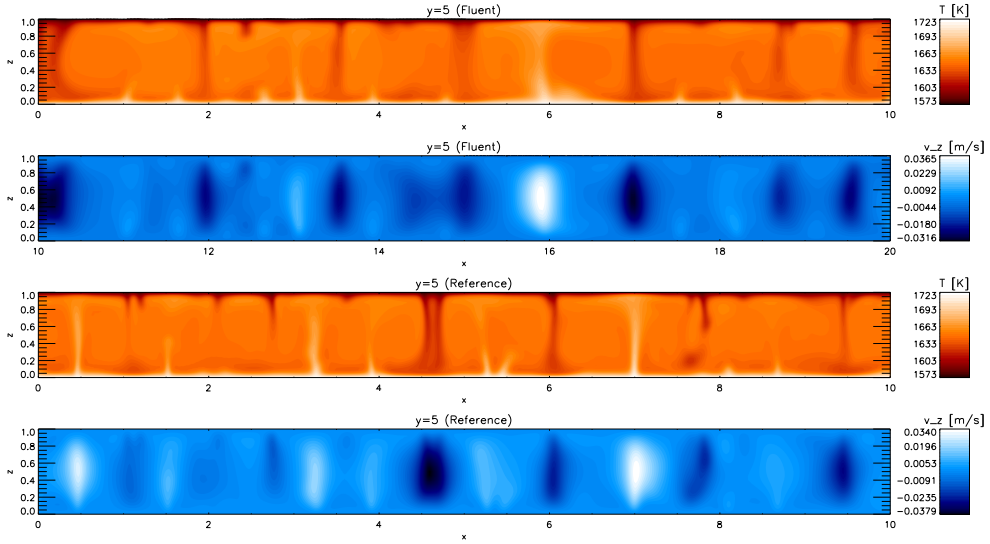

FIGURE 4. Horizontal slices at $y = 5\,\mathrm{m}$ of the temperature and vertical velocity in the Fluent simulation (*top*) and in the reference simulations (*bottom*).

flow where plumes persist for much longer times. The average separation between these longer-lived structures is about 4 m in this case, which is consistent with experiments (for a compilation of simulations and experimental data at different Ra and Pr, see Hartlep et al. 2005). The fact that the time scales of the different features in the flow differ is of course lost in a steady state simulation, like the one performed with Fluent. Such details could be important when, for instance, estimating typical mixing times from simulation. For comparison, we have also performed a Fluent simulation at a lower resolution (1.5 M cells) of which results are shown in figure 3. This case is clearly under-resolved, and the plumes are significanly thicker compared to the cases shown in figures 1 and 2. However, the heat flux through the system seems to be rather insensitive to the reduced resolution, as the xy-averaged temperature is very close to what is found by the reference simulation (see figure 3, right panel). Finally, we show vertical cuts of the temperature and velocity for the high-resolution Fluent case and a snapshot of the reference simulation (figure 4). The temperature shows the structure of the very slender thermal plumes with their typical mushroom-like heads. It can be seen that they routinely reach all the way from one boundary layer to the other. As evidenced by the velocity plots, the up- and down-flows are much wider than the thermal structures. This can be attributed to the large Prandtl number of the fluid.

4. Conclusions

The usefulness of steady state simulations using Fluent has been assessed for a problem of interest to the glass industry. It has been found that many aspects of the flow are accurately represented by the high resolution (6.25M cells) Fluent simulation, such as the small scale structure of spokes and convective plumes and the thickness of the boundary layers. Since the actual flow is not totally stationary, as seen from the time-dependent reference simulation, some aspects are lost, though. For instance, the large scale organization of the plume network is not clearly visible in the Fluent simulation.

As a next step, we plan to use a more realistic and temperature-dependent viscosity for the glass as well as a thermal diffusivity accounting for radiation.

REFERENCES

Busse, F. H. 1967 On the stability of two-dimensional convection in a layer heated from below. *J. Math. Phys. Mech.* **46**, 140–150.

Busse, F. H. 1979 High Prandtl number convection. *Phys. of the Earth and Planet. Interiors* **19**, 149–157.

Busse, F. H. & Whitehead, J. A. 1974 Oscillatory and collective instabilities in large Prandtl number convection. *J. Fluid Mech.* **66**, 67–79.

Chiu-Webster, S., Hinch, E. J. & Lister, J. R. 2008 Very viscous horinzontal convection. *J. Fluid Mech.* **611**, 395–426.

Clever, R. M. & Busse, F. H. 1974 Transition to time-dependent convection. *J. Fluid Mech.* **65**, 625–645.

Clever, R. M. & Busse, F. H. 1987 Nonlinear oscillatory convection. *J. Fluid Mech.* **176**, 403–417.

Clever, R. M. & Busse, F. H. 1994 Steady and oscillatory bimodal convection. *J. Fluid Mech.* **271**, 103–118.

Flesselles, J.-M., Pigeonneau, F. 2004 Kinematic regimes of convection at high Prandtl number in a shallow cavity. *C. R., Mécanique.* **332**, 783-788, 2004.

Frick, H., Busse, F. H. & Clever, R. .M. 1983 Steady three-dimensional convection at high Prandtl number. *J. Fluid Mech.* **127**, 141–153.

Hansen, U., Yuen, D., A. & Kroening, S. E. 1990 Transition to hard turbulence in thermal convection at infinite Prandtl number. *Phys. Fluids. A* **2**, 2167.

Hartlep, T., Tilgner, A. & Busse, F. H. 2003 Large scale structures in Rayleigh-Bénard convection at high Rayleigh numbers. *Phys. Rev. Letters* **91**(6), 64501.

Hartlep, T. & Tilgner, A. 2003 Rayleigh-Bénard convection at large aspect ratios. *High Performance Computing in Science and Engineering '03.* Springer Verlag.

Hartlep, T., Tilgner, A. & Busse, F. H. 2005 Transition to turbulent convection in a fluid layer heated from below at moderate aspect ratio. *J. Fluid Mech.* **554**, 309–322.

Kerr, R. M. 1996 Rayleigh number scaling in numerical convection. *J. Fluid Mech.* **310**. 139–179.

Koschmieder, E. L. 1993 *Bénard cells and Taylor vortices.* Cambridge University Press.

Moser, R. D., Moin, P. & Leonard, A. 1983 A spectral numerical method for the Navier Stokes equations with application to Taylor Couette flow. *J. Comp. Phys.* **54**, 524–544.

Pillon, L., Zhao, G. & Viskanta, R. 2002 Three-dimensional flow and thermal structures in glass melting furnaces. *Glass Sci. Technol.* **75**(2), 55–68.

Rossby., T. 1965 On thermal convection driven by non-uniform heating from below; an experimental study. *Deep-sea Res.* **12**, 9–16.

Stein, R. F. & Nordlund, A. 1998 Simulations of solar granulation: I. General properties. *ApJ.* **499**, 914-933.

Stein, R. F., Nordlund, A., Ripoll, J.-F. & Wray A. A. 2004 Solar surface convection. *Proceed. CTR Summer Prog.* 21-31.

Wang W. & Huang, R. X. 2005 An experimental study on thermal circulation driven by horizontal differential heating. *J. Fluid Mech.* **540**, 49–73.